*applied sciences*

MDPI

*Article*

# DTW-kNN and Sentinel-2 NDVI Time Series for Field-Scale Maize Identification and Multi-Crop Classification in an African Smallholder Landscape

**Wonga Masiza [1,*], Pitso Walter Khoboko [2] and Johannes George Chirima [1,3]**

[1] Geoinformatics Division, Agricultural Research Council-Natural Resources and Engineering, Arcadia 0083, South Africa
[2] Neria Solutions, 21354, Turflaagte 2, Bloemfontein 9323, South Africa
[3] Centre for Geoinformation Science, Department of Geography, Geoinformatics, and Meteorology, University of Pretoria, Pretoria 0001, South Africa
* Correspondence: masizaw@arc.agric.za

**Abstract**

Mapping crops at the field scale supports agricultural planning, production monitoring and resource allocation. However, this remains difficult in smallholder landscapes, where planting dates vary among farms, ground-reference data are limited, and fields are small, fragmented and irregularly shaped. This study evaluated Sentinel-2 Normalised Difference Vegetation Index (NDVI) time series combined with Dynamic Time Warping k-nearest neighbour (DTW-kNN) for maize identification and multi-crop classification in the O.R. Tambo District Municipality, South Africa.. A maize reference trajectory was first developed from known maize fields and then assessed against independent maize validation fields and candidate unknown fields. Known maize fields produced low DTW distances to the maize reference trajectory, while Days After Planting alignment showed a clear maize phenological pattern, with NDVI increasing after planting, peaking between approximately 90 and 120 DAP, and declining thereafter. For multi-crop classification, a simple mean-reference DTW baseline achieved 80.0% accuracy on independent validation fields. Retaining individual reference-field trajectories (DTW-kNN) instead of a single mean reference improved on this baseline. Training-only cross-validation selected DTW-kNN with k = 1 and a one-composite warping window; this configuration achieved 92.9% independent validation accuracy, comparable to benchmark Random Forest and Support Vector Machine classifiers (95.7%). DTW-kNN remained competitive while retaining direct temporal-similarity interpretation. When applied to 128 unlabelled fields, the selected DTW-kNN classifier predicted 106 fields as maize and 22 as soybean, with 65.6% of predictions classified with high confidence. The findings show that Sentinel-2 NDVI time series combined with DTW-kNN can support interpretable field-level crop classification in fragmented smallholder farming systems.

**Keywords:** Sentinel-2; NDVI time series; dynamic time warping; DTW-kNN; maize identification; crop classification; smallholder agriculture

Check for updates

Academic Editor: Rui Sun

Received: 22 July 2026
Revised: 22 September 2026
Accepted: 29 September 2026
Published: 9 November 2026

**Copyright:** © 2026 by the authors. Licensee MDPI, Basel, Switzerland. This article is an open access article distributed under the terms and conditions of the Creative Commons Attribution (CC BY) license.

## 1. Introduction

Crop mapping is the process of identifying and categorising the spatial distribution of cultivated crops across agricultural landscapes [1]. This process is important because it shifts agricultural information from administrative estimates and self-reported statistics towards

direct, spatially explicit measurement [2,3]. By showing where specific crops are grown, crop mapping provides the spatial basis for estimating cultivated area, monitoring seasonal crop development, assessing production potential, and linking field-level observations with broader regional or national agricultural statistics [4]. This information is valuable for policymakers who need reliable evidence to support agricultural planning, food-system monitoring, and resource allocation [5–7]. It is also important for agribusinesses, which rely on spatially explicit crop information to optimise supply chains, identify investment opportunities, and manage production and market-related risks [8]. The need for accurate crop mapping has become even more pressing under changing climatic conditions, which affect crop growth, planting calendars, and yield stability [9]. This urgency is compounded by a growing global population, which places increasing demands on agricultural land and production systems [10–12].

Nevertheless, the mapping and monitoring of crops in smallholder farming areas remains difficult. This difficulty is mainly due to fragmented, small and irregularly shaped fields [13–15], and varying planting dates [16–18], compounded by cloud cover, which limits the availability of usable optical satellite imagery during the growing season [19]. Since smallholder farmers often plant at different times, even within the same locality, crop identification cannot rely on single-date imagery or same-date comparisons between fields. For instance, two maize fields may be at different growth stages on the same image acquisition date, while different crops may appear similar during certain parts of the season. This temporal variability complicates crop classification and motivates the use of time-series methods that can compare the overall shape of crop development trajectories rather than only their values at fixed dates [20].

Dynamic Time Warping (DTW) is a time series similarity method that can compare temporal sequences even when similar patterns occur at different times or progress at different rates [21,22]. This makes DTW particularly suitable for agricultural applications where planting dates, crop growth rates, and senescence timing differ among fields. Vegetation indices such as the Normalised Difference Vegetation Index (NDVI) are widely used to describe crop growth because they respond to changes in green biomass, canopy cover and phenological development [23,24]. By extracting NDVI observations across the growing season, it is possible to construct temporal trajectories that describe crop establishment, canopy expansion, peak greenness and senescence [25,26]. Instead of requiring two NDVI curves to match point by point on the same calendar dates, DTW allows local stretching and compression of the time axis to identify similarity in the overall temporal pattern [21,22]. This is particularly relevant for crop mapping in smallholder systems where planting-date variability is common and large training datasets are often unavailable [27–29].

Beyond DTW, a range of other approaches has been applied to time-series-based crop mapping. Conventional machine-learning methods, such as Random Forest (RF), Support Vector Machine (SVM) and k-nearest neighbour (kNN) classifiers, are widely used because they can learn class-separating patterns from multi-temporal spectral features [1,10,20,30–32]. More recently, deep-learning approaches have also been applied to crop-type mapping because they can model complex temporal patterns in image time-series [33–38]. However, these methods often require larger training datasets, careful model tuning and additional interpretation procedures to explain how crop classes are separated [1,35,38–42]. Similarity-based approaches such as DTW offer a complementary alternative because they classify fields by comparing their temporal trajectories with known crop-growth patterns [1]. This makes DTW particularly relevant where labelled field data are limited and where interpretable phenological matching is important.

Despite growing interest in time-series crop classification, the application of DTW-based methods to maize identification and multi-crop field-boundary classification in fragmented smallholder landscapes remains limited, especially in Africa. Existing studies from

Asia, Europe and North America have shown that DTW and related time-series approaches can support crop mapping under variable crop calendars, limited training data and complex phenological patterns [29,43–46]. Much of the existing DTW-based crop mapping literature has focused on rice systems, wheat mapping, crop-intensity mapping, broad cropland extraction, or commercial and intensively managed agricultural landscapes [27,47–50]. Less attention has been given to testing whether simple mean-reference DTW, improved DTW-kNN configurations and conventional machine-learning classifiers perform differently when applied to smallholder fields with limited reference data and variable planting dates. This gap is important because crop-mapping methods for smallholder systems must balance classification accuracy, reference-data requirements and interpretability.

This study therefore evaluated Sentinel-2 NDVI time series and DTW-based approaches for maize identification and multi-crop field-boundary classification in the O.R. Tambo District Municipality, South Africa during the 2025/26 growing season. The study addressed five research questions: (i) Can Sentinel-2 NDVI time series and DTW identify maize fields despite variable planting dates? (ii) Does Days After Planting (DAP) alignment provide a meaningful representation of maize phenology? (iii) Can calendar-date DTW classify field polygons into maize, soybean, potato and tea in a smallholder landscape? (iv) Does classification performance improve when DTW is implemented as a reference-field k-nearest neighbour classifier with constrained temporal warping? and (v) how does the selected DTW-based classifier compare with conventional machine-learning classifiers trained on the same Sentinel-2 NDVI time-series features?

The specific objectives were to: (i) develop and validate a maize NDVI reference trajectory for DTW-based maize identification; (ii) assess maize phenological development by aligning NDVI observations according to DAP; (iii) develop crop-specific NDVI reference trajectories for maize, soybean, potato and tea; (iv) evaluate simple mean-reference DTW and DTW-kNN configurations for multi-crop field-boundary classification; (v) compare the selected DTW-based classifier with conventional machine-learning benchmark models; and (vi) apply the selected DTW-based classifier to unknown field polygons to generate field-level crop predictions and DTW confidence classes.

## 2. Materials and Methods

### *2.1. Study Area*

The study was conducted in the O.R. Tambo District Municipality (ORTDM) located in the Eastern Cape Province of South Africa (Figure 1).

The area has five local municipalities, namely: Mhlontlo, Ingquza Hill, Nyandeni, Port St Johns, and King Sabata Dalindyebo. The dominant agricultural activity is smallholder crop farming, mainly involving maize, followed by soybean, potato, tea and leafy vegetables grown in smaller fields, often less than one hectare [17]. Maize, potato and soybean are cultivated on communal lands, with cultivated holdings ranging from less than one hectare to several hundred hectares, often planted between August and January, while tea is a perennial crop grown in the well-known Magwa Tea Estate [14,51,52]. The tea plantations consist of the evergreen plant, *Camellia sinensis*, which is a perennial shrub that is continually harvested and can live and produce for decades. Potatoes are harvested between December and April, while maize and soybeans are harvested between May and July.

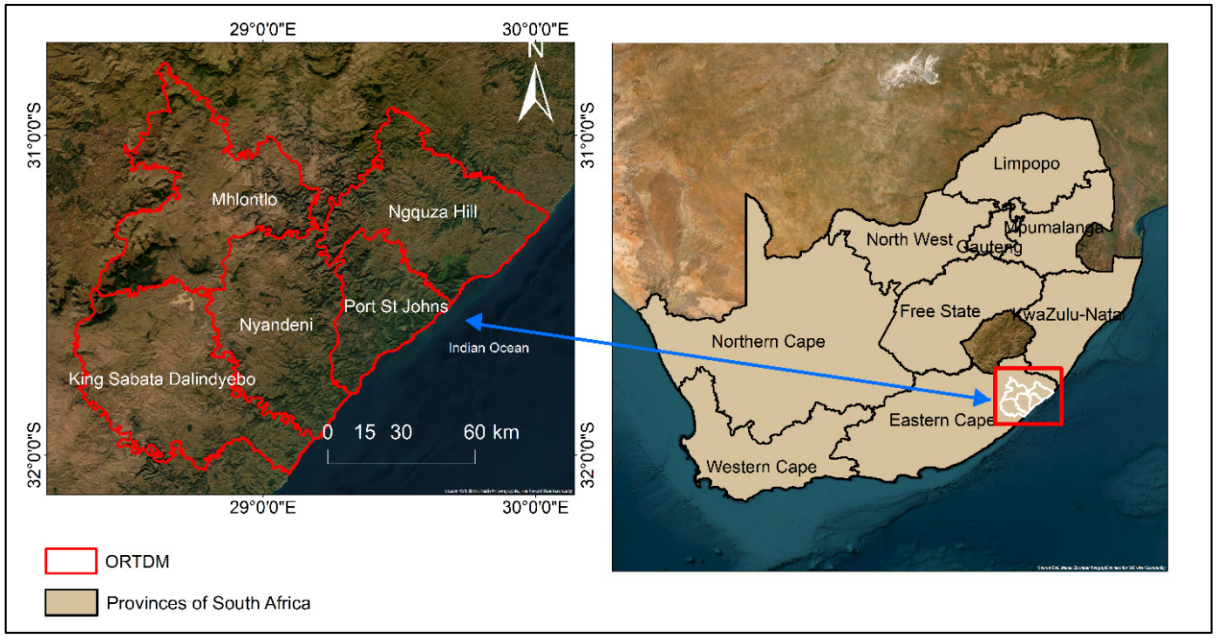



**Figure 1.** Study area map showing the location of ORTDM.

Driven by its coastal positioning, diverse terrain, and distinct climatic shifts, the district supports a varied ecological landscape. While the coastal fringe is characterised by dense thickets and woody vegetation, the interior transitions into a landscape dominated by grasslands and savannas [53]. Climatically, the region shifts from a humid, subtropical coastal zone to a more temperate, semi-dry inland plateau [54]. Rainfall is highly seasonal, concentrated between October and March, yielding 800–1200 mm annually near the sea and dropping to 600–900 mm further inland. Temperatures near the coast remain moderate throughout the year, averaging summer highs of 24–30 °C and winter lows of 8–12 °C. Conversely, the interior experiences sharper seasonal fluctuations, with summer temperatures reaching 30 °C and winter nights dropping to between 3 and 5 °C.

The Eastern Cape Province, particularly the O.R. Tambo District Municipality, is a suitable study area for small-scale crop mapping because it contains South Africa's largest concentrations of smallholder farmers, who cultivate maize under highly fragmented and rainfed conditions [55]. Furthermore, it is characterised by variable planting dates and frequent cloud-related observation challenges. The methods and findings from this study therefore have potential relevance for other smallholder crop-farming areas with fragmented fields, variable planting dates and cloud-related observation challenges.

### *2.2. Analytical Workflow*

The analysis followed a staged field-boundary time-series classification workflow. First, field-boundary and crop-reference data were prepared for maize-only and multi-crop analyses. Second, Sentinel-2 Level-2A imagery was used to generate 10-day NDVI composite time series for each field polygon. Third, missing values in the field-level NDVI trajectories were filled using linear interpolation, and Whittaker smoothing was applied to the maize-only reference trajectory and maize DAP phenology analyses. Fourth, a maize reference trajectory was developed from known maize fields and evaluated using independent maize validation fields and candidate unknown fields. Fifth, maize phenology was examined by converting calendar-date observations into DAP. Sixth, the analysis was extended to multi-crop field-boundary classification using maize, soybean, potato and tea reference trajectories. Finally, DTW sensitivity tests, DTW-kNN classification and conventional machine-learning

benchmark models were used to evaluate whether more robust classification approaches improved performance compared with simple mean-reference DTW (Figure 2).

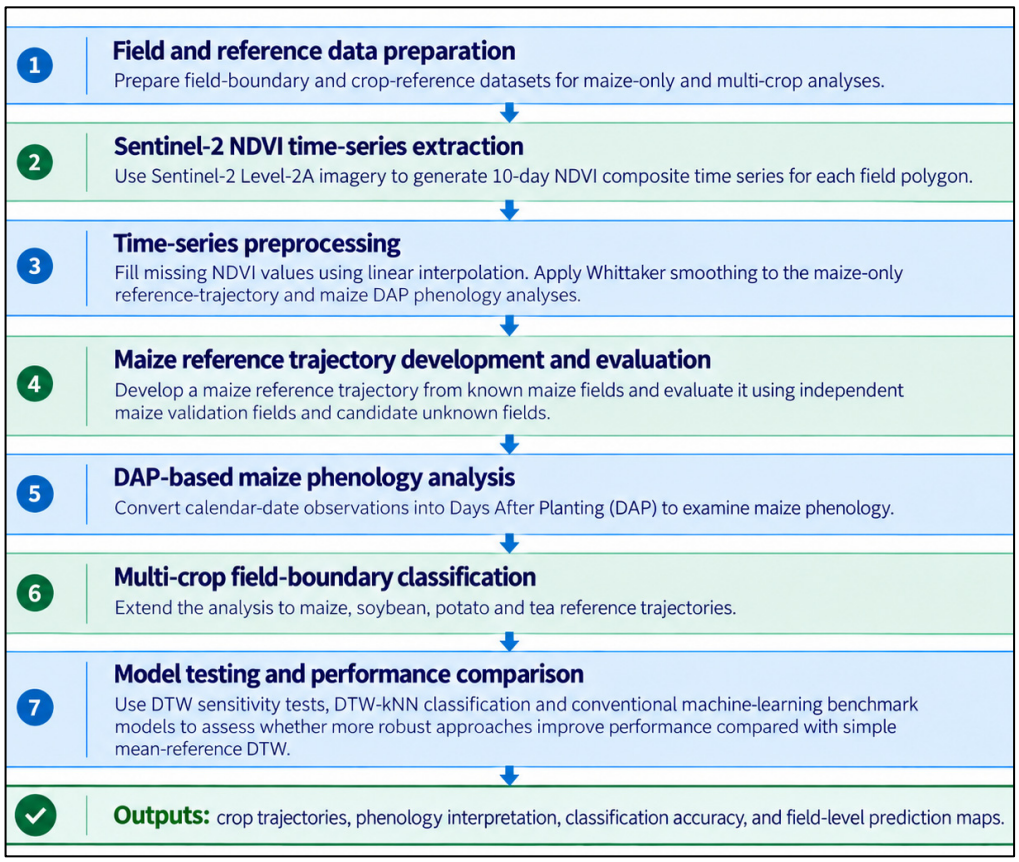



**Figure 2.** Overview of analytical workflow.

### *2.3. Field Reference Data*

The study used field-boundary polygons representing known and unknown crop fields during the 2025/26 growing season. Field polygons were used as the basic spatial unit of analysis because they represent agricultural management units and allow satellite-derived NDVI values to be summarised at field level. Field polygons retained for analysis ranged from approximately 0.5 ha to more than 7 ha. Very small or narrow polygons were excluded where their geometry was considered unsuitable for reliable extraction of field-level NDVI values from 10 m Sentinel-2 imagery. Two related datasets were used: one for maize reference-trajectory development and DAP analysis, and another for multi-crop field-boundary classification.

#### 2.3.1. Maize Reference-Trajectory and DAP Field Dataset

The maize reference-trajectory analysis used 28 known maize fields with recorded planting dates. These fields were distributed across the ORTDM, representing different cultivation areas, cultivars, and planting dates. The planting dates ranged from October to January, capturing the planting-time variability commonly observed among smallholder farms in South Africa [17,56–59]. The maize cultivars were varieties of Pannar, Dekalb, Lima Green, and unbranded open-pollinated seeds.

The 28 known maize fields were divided into two groups. The first group consisted of 19 maize fields used to develop the representative maize NDVI reference trajectory for the DTW analysis. The second group consisted of nine independent maize fields reserved for validation. These validation fields provided an independent test of whether the maize

reference trajectory could generalise to unseen maize fields. Since DAP analysis requires known planting dates, the 28 known maize fields were used to construct the crop-age-aligned maize phenology curve (Table 1).

**Table 1.** Maize reference-trajectory, validation and candidate-field datasets.

| Dataset | Number of Fields | Purpose |
|---|---|---|
| Maize reference fields | 19 | Develop the maize reference trajectory |
| Independent maize validation fields | 9 | Test whether the maize reference trajectory generalises to unseen fields |
| Candidate unknown fields | 31 | Assess maize-like phenological behaviour among unlabelled fields |

In addition to the known maize fields, 31 candidate fields of unknown crop type were digitised from Sentinel-2 imagery. These fields were selected because they showed visual and seasonal vegetation characteristics similar to known maize fields, including field shape, texture and seasonal greening patterns. The candidate fields were not used to develop the maize reference trajectory. Instead, they were used to test whether the maize reference trajectory could identify additional fields with maize-like phenological behaviour (Table 1).

#### 2.3.2. Multi-Crop Field-Boundary Classification Dataset

The multi-crop field-boundary classification used a larger dataset of 342 field polygons. This dataset included 93 maize fields, 42 soybean fields, 28 potato fields, 51 tea fields and 128 fields of unknown crop type. The known fields were used for reference-trajectory development, DTW parameter testing and independent validation, while the unknown fields were reserved for prediction and mapping (Table 2).

**Table 2.** Multi-crop field dataset used for classification, validation and prediction.

| Use | Maize | Soybean | Potato | Tea | Unknown |
|---|---|---|---|---|---|
| Reference | 63 | 28 | 18 | 35 | 0 |
| Validation | 30 | 14 | 10 | 16 | 0 |
| Prediction | 0 | 0 | 0 | 0 | 128 |
| Total | 93 | 42 | 28 | 51 | 128 |

The reference group consisted of 144 fields, including 63 maize, 28 soybean, 18 potato and 35 tea fields. These fields were used to develop crop-specific NDVI reference trajectories and to conduct training-only cross-validation for DTW-kNN parameter selection. The independent validation group consisted of 70 fields, including 30 maize, 14 soybean, 10 potato and 16 tea fields. These validation fields were excluded from reference-trajectory development and parameter selection and were used only for final accuracy assessment (Table 2).

The 128 unknown fields had no confirmed crop labels and were therefore excluded from accuracy assessment. They were used to evaluate the operational applicability of the DTW-based classification framework. Each unknown field was compared with the crop reference data and assigned to the crop class with the strongest temporal similarity. The outputs were interpreted as field-level predictions rather than independently validated crop labels. The 128 unknown fields were located within an intensely cultivated sub-area of the ORTDM, covering approximately 10 km × 10 km. This sub-area was selected because it

contained a high concentration of digitised crop fields and provided a practical test area for applying the multi-reference DTW classifier to unlabelled field polygons. The resulting predictions should therefore be interpreted as field-level classifications within this selected cultivated zone, rather than as a wall-to-wall crop map for the entire district.

### 2.4. Sentinel-2 NDVI Time-Series Extraction Using Google Earth Engine

Sentinel-2 Level-2A Surface Reflectance imagery was used to generate field-level NDVI time series for all field polygons. The imagery was obtained from the Copernicus Sentinel-2 Harmonized archive in Google Earth Engine (GEE) [60]. Sentinel-2 was selected because its 10 m red and near-infrared bands are suitable for monitoring seasonal vegetation development in smallholder agricultural fields [61,62].

Two temporal windows were used to match the analytical requirements of the study. For the maize reference-trajectory and DAP analysis, imagery from October 2025 to May 2026 was used. This period corresponded to the main maize growing season, encompassing establishment, canopy development, peak greenness and senescence. For the multi-crop field-boundary classification, the extraction period was from 1 August 2025 to 31 May 2026, to accommodate the earlier planting and longer growth cycle of potato.

Cloud-affected and invalid pixels were removed using the Sentinel-2 Scene Classification Layer (SCL). Pixels classified as no-data, saturated or defective, cloud shadow, medium-probability cloud, high-probability cloud, cirrus, snow or ice were excluded. Sentinel-2 scenes with less than 70% scene-level cloud cover were retained. This relatively relaxed scene-level threshold was used to maximise temporal coverage during the cloudy periods of the growing season, while the pixel-level SCL mask was used to remove cloud-contaminated pixels within each image.

NDVI was calculated for each valid Sentinel-2 observation using the red (Band 4) and near-infrared (Band 8) bands [23,24]. The image collection was then aggregated into consecutive 10-day composite periods. For each 10-day interval, the median NDVI value was calculated from all valid observations available within that period. Median compositing was used to reduce the influence of residual cloud contamination, atmospheric noise and anomalous observations while preserving the seasonal pattern of crop development.

Field-level NDVI values were extracted by calculating the mean NDVI within each field polygon for every 10-day composite period. This converted the satellite imagery into a field-by-date time-series matrix, where each row represented a field polygon and each column represented a 10-day NDVI composite. The maize reference-trajectory analysis produced a 22-period NDVI trajectory for each field, while the multi-crop classification produced a 31-period trajectory for each field because of the longer extraction window. The same 31-period field-level NDVI features were used for the simple mean-reference DTW classifier, the DTW-kNN sensitivity analysis and the conventional machine-learning benchmark models.

### 2.5. Time-Series Preprocessing and Analysis in Python

The field-level NDVI time-series outputs from GEE were imported into Python version 3.11.3 and analysed using Jupyter Notebook version 6.5.4. Data preparation and reshaping were performed using pandas version 2.3.1 and NumPy version 2.3.2, while figures were generated using matplotlib version 3.10.5. DTW distances were calculated using the dtaidistance version 2.4.0 Python package. Whittaker smoothing was implemented using the whittaker-eilers version 0.2.0 package, and machine-learning benchmark models and accuracy metrics were implemented using scikit-learn version 1.7.1.

Missing NDVI values were filled using linear interpolation along each field's temporal profile [63]. Linear interpolation estimated missing values from the nearest valid observa-

tions before and after the missing period, thereby producing continuous NDVI trajectories required for DTW comparison. For the maize reference-trajectory and maize DAP phenology analysis, the interpolated NDVI trajectories were further smoothed using a Whittaker filter [64]. The Whittaker smoother was applied using a smoothing parameter of $\lambda = 10$ and a second-order difference penalty. The purpose of smoothing was to reduce short-term fluctuations while preserving the main phenological features of maize development, including crop establishment, canopy expansion, peak greenness and senescence.

For the multi-crop field-boundary DTW classification, no additional Whittaker smoothing filter was applied. The multi-crop analysis used the linearly interpolated 31-period NDVI trajectories so that the simple mean-reference DTW classifier, DTW-kNN sensitivity analysis and machine-learning benchmark models were evaluated using the same input features. Whittaker smoothing was therefore used only for the maize reference-trajectory and DAP phenology analyses, where the objective was to describe the main seasonal maize growth pattern rather than to optimise multi-crop classification.

No additional scaling or normalisation was applied before the DTW analyses. The DTW comparisons were based on NDVI time series, and all time-step values were measured on the same NDVI scale. For the machine-learning benchmark models, standardisation was applied only to algorithms that are sensitive to feature scale, namely SVM, distance-weighted kNN and Ridge Classifier [65]. No feature scaling was applied to the RF model.

### 2.6. Maize Reference-Trajectory Development and DAP Analysis

The maize reference-trajectory analysis was conducted to evaluate whether known maize fields followed a recognisable Sentinel-2 NDVI temporal pattern that could be used for DTW-based maize identification. A mean maize reference trajectory was then calculated by averaging the smoothed NDVI values of the 19 reference fields at each 10-day composite period. This mean trajectory represented the typical seasonal NDVI pattern of maize in the study area, including early establishment, canopy development, peak greenness and senescence. DTW was then used to compare each field-level NDVI trajectory with the maize reference trajectory. DTW calculates the temporal dissimilarity between two time series while allowing limited differences in the timing of comparable phenological stages [21,22,29,66]. Lower DTW distances indicate greater similarity to the maize reference trajectory, whereas higher distances indicate weaker similarity.

The DAP analysis was conducted using all 28 known maize fields with recorded planting dates. For each field and composite period, DAP was calculated as the difference between the Sentinel-2 composite date and the field planting date. Negative DAP values, representing observations before planting, were excluded. The remaining observations were grouped into 10-day DAP intervals, and the mean, median and number of observations were calculated for each interval. This converted the maize NDVI time series from calendar-date alignment to crop-age alignment, allowing maize phenological development to be assessed independently of differences in planting date. Observation support was reported as the number of field-date NDVI observations contributing to each DAP interval, rather than the number of unique fields.

### 2.7. Multi-Crop DTW Classification and Sensitivity Analysis

The multi-crop classification analysis was conducted to evaluate whether Sentinel-2 NDVI temporal trajectories could distinguish maize from soybean, potato and tea at field-boundary scale. The analysis used the 31-period calendar-date NDVI trajectories generated between 1 August 2025 and 31 May 2026. Classification was first conducted using a simple mean-reference DTW approach, after which additional DTW variants were tested to assess

whether classification performance improved when within-class variability and constrained temporal warping were considered.

#### 2.7.1. Simple Mean-Reference DTW Classification

For the initial multi-crop DTW classification, a crop-specific mean NDVI reference trajectory was developed for each class using the 144 reference fields. The reference group included maize, soybean, potato and tea fields. For each crop class, the mean NDVI value was calculated at each 10-day composite period across all reference fields belonging to that class. This produced one representative NDVI trajectory for each crop type.

Each validation field was then compared with the four crop-specific reference trajectories using DTW. The DTW distance between the validation field trajectory and each crop reference trajectory was calculated, and the field was assigned to the crop class with the lowest DTW distance. Lower DTW distances indicated greater similarity between the observed field trajectory and the crop reference trajectory. This simple mean-reference approach was used as the baseline DTW classifier.

#### 2.7.2. DTW-kNN Classification and Warping-Window Sensitivity

To test whether DTW performance improved when individual reference-field trajectories were retained, a DTW-kNN approach was also evaluated. Unlike the mean-reference DTW approach, which compares each field with one average trajectory per crop, DTW-kNN compares each validation field with all individual reference-field trajectories. The predicted crop class is then assigned based on the closest reference trajectory or the majority class among the nearest reference trajectories.

Several DTW-kNN configurations were tested by varying the number of nearest neighbours and the warping-window constraint. The number of neighbours was tested using $k = 1, 3, 5$ and 7. The warping-window settings included unconstrained DTW and constrained windows of 1, 2, 3, 4 and 5 composite periods. The constrained warping windows limited the amount of temporal shifting allowed during DTW matching. This was done to prevent unrealistic alignments between crop growth stages while still allowing some flexibility in the timing of crop development.

#### 2.7.3. Training-Only Parameter Selection

To avoid selecting DTW parameters using the independent validation data, DTW-kNN parameter selection was conducted using five-fold cross-validation within the 144 reference fields. During this procedure, the reference fields were repeatedly split into internal training and testing folds. For each combination of k and warping-window size, DTW-kNN predictions were generated for the held-out fold and classification performance was recorded.

The DTW-kNN configuration with the highest cross-validated performance was selected as the final DTW-based classification approach. This selected configuration was then evaluated once using the 70 independent validation fields.

#### 2.7.4. DAP-Aligned Multi-Crop DTW Experiment

An additional DAP-aligned DTW experiment was conducted to test whether crop-age alignment improved multi-crop classification among annual crops. This experiment was separate from the calendar-date DTW-kNN workflow used for final classification. It was restricted to maize, soybean and potato fields with recorded planting dates. Tea was excluded because it is a perennial crop and does not have a comparable annual planting date.

Crop-specific DAP reference trajectories were developed from the reference fields by calculating the mean NDVI of each crop class at each DAP interval. Validation fields were converted to the same DAP-aligned format and classified by comparing their DAP-

based NDVI trajectories with the crop-specific DAP reference trajectories using DTW. Each validation field was assigned to the crop class with the lowest DTW distance.

Two DAP-DTW variants were evaluated: one using the full available DAP-aligned trajectory for each field, and another restricted to the 0–160 DAP period to test whether classification improved when the comparison was limited to a common early-to-mid-season crop-age window. Classification accuracy was then assessed using the same validation metrics applied to the calendar-date multi-crop DTW analysis.

#### 2.7.5. Unknown-Field Prediction and DTW Confidence Assessment

After selecting the final DTW-kNN configuration, the model was applied to the 128 unknown field polygons. These polygons were used only to evaluate the operational applicability of the DTW-based classification workflow to unlabelled field boundaries.

Each unknown field was compared with all 144 reference fields using DTW-kNN with k = 1 and a one-composite warping window. The crop class of the closest reference field was assigned as the predicted class. In addition, the minimum DTW distance between each unknown field and each crop class was calculated. The difference between the lowest and second-lowest class-level DTW distances was used as the DTW margin.

The DTW margin was used as a practical indicator of classification confidence. Fields with a margin of 0.15 or greater were classified as high confidence, fields with a margin between 0.07 and 0.15 were classified as moderate confidence, and fields with a margin below 0.07 were classified as low or uncertain confidence. These confidence classes were used to indicate the degree of separation between the best-matching crop class and the next-best alternative. They should not be interpreted as calibrated probabilities. The unknown-field predictions were mapped together with DTW confidence classes to show the spatial distribution of predicted crop types within the selected cultivated sub-area.

### *2.8. Machine-Learning Benchmark Classifiers*

Conventional machine-learning classifiers were implemented as benchmark models to compare DTW-based classification with commonly used supervised classification approaches. The benchmark models were trained using the same 31-period Sentinel-2 NDVI time-series features used in the multi-crop DTW analysis. Four benchmark classifiers were evaluated. RF [67,68] was included as a tree-based ensemble classifier that can model non-linear relationships in the NDVI time-series features. SVM [69,70] with a radial basis function kernel was included to test whether a margin-based classifier could separate crop classes in the multi-temporal NDVI feature space. A distance-weighted kNN classifier [71–73] was included as a feature-space nearest-neighbour benchmark. Ridge Classifier [74] was included as a regularised linear benchmark.

Standardisation was applied to the SVM, distance-weighted kNN and Ridge Classifier models because these algorithms are sensitive to feature scale [65]. RF was fitted without feature scaling. For reproducibility, RF was fitted using 500 trees, class weighting and square-root feature selection; the SVM used a radial basis function kernel; the feature-space kNN model used five distance-weighted neighbours; and Ridge Classifier was fitted with class weighting.

### *2.9. Accuracy Assessment*

Accuracy assessment was conducted separately for the maize-only DTW analysis, the multi-crop DTW classification and the machine-learning benchmark models. For the maize-only reference-trajectory analysis, the independent maize validation fields were compared with the mean maize reference trajectory using DTW distance. Because this stage focused only on maize similarity rather than multi-class crop discrimination, the assessment was

based on the range and distribution of DTW distances obtained from the independent maize validation fields.

For the multi-crop classification analysis, accuracy assessment was based on the independent validation fields, which included maize, soybean, potato and tea. Classification performance was assessed using a confusion matrix, overall accuracy, balanced accuracy, Cohen's kappa, class-specific precision, recall and F1-score, macro-averaged F1-score and weighted F1-score [75]. Overall accuracy measured the proportion of correctly classified validation fields. Balanced accuracy was included because the number of validation fields differed among crop classes. Cohen's kappa was used to assess agreement between observed and predicted crop classes after accounting for chance agreement. Precision, recall and F1-score were used to evaluate class-level performance, while macro-F1 and weighted-F1 summarised performance across all crop classes.

For unknown-field prediction, no accuracy statistics were calculated because the 128 prediction fields had no confirmed crop labels. These fields were therefore summarised only by predicted crop class and DTW confidence category. The DTW confidence categories were based on the margin between the lowest and second-lowest class-level DTW distances and were interpreted as practical indicators of classification separation, not as calibrated probabilities.

## 3. Results

### *3.1. Maize Reference Trajectory and DTW-Based Maize Similarity*

The maize reference trajectory showed a clear seasonal NDVI pattern consistent with maize establishment, canopy development, peak greenness and senescence. The 19 maize reference fields produced similar but not identical temporal profiles, reflecting differences in planting dates, local field conditions and crop management. After interpolation and Whittaker smoothing, the mean maize reference trajectory provided a representative seasonal NDVI curve against which validation and candidate fields could be compared (Figure 3).

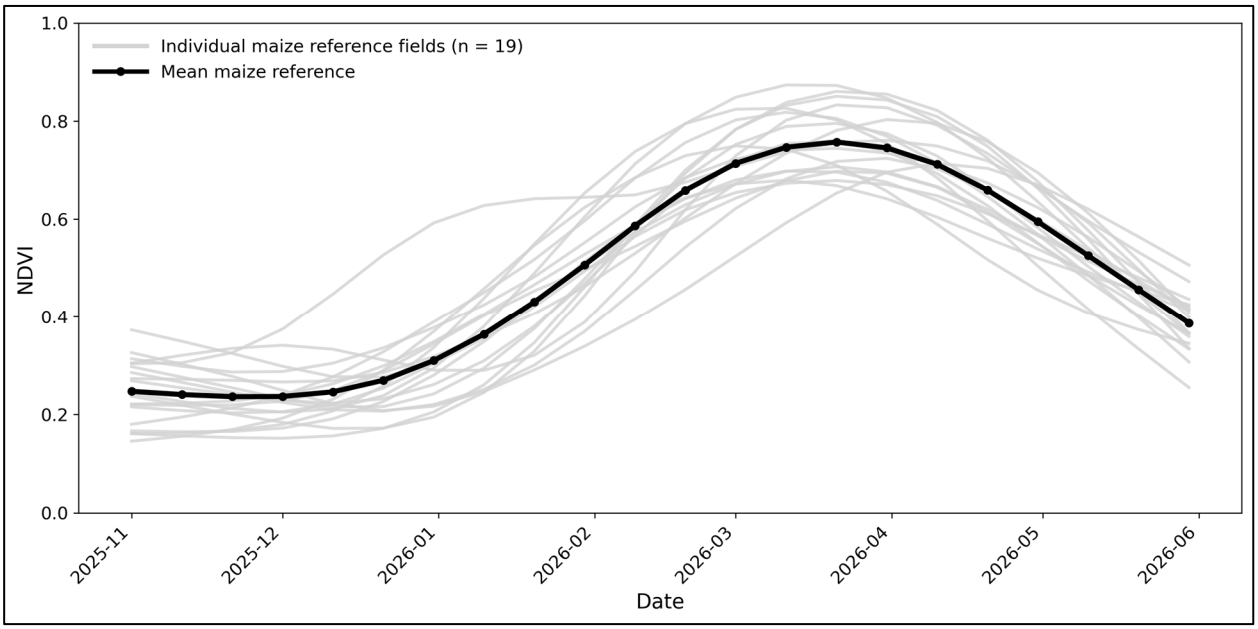



**Figure 3.** Smoothed NDVI trajectories of maize reference fields and the mean maize reference trajectory.

The DTW distances for the 19 maize reference fields ranged from 0.106 to 0.281, indicating that the reference fields showed broadly similar maize-like temporal behaviour (Table 3).

**Table 3.** DTW distance ranges for maize reference, validation and candidate fields.

| Field Group | Number of Fields | DTW Distance | Interpretation |
|---|---|---|---|
| Maize reference fields | 19 | 0.106–0.281 | Known maize fields were similar to the maize reference |
| Independent maize validation fields | 9 | 0.074–0.325 | Independent maize fields were also similar to the reference |
| Candidate unknown fields | 31 | 0.151–0.565 | Some candidates were maize-like; others were less similar |

The nine independent maize validation fields produced DTW distances ranging from 0.074 to 0.325. This validation-distance range was used as a practical benchmark for interpreting maize-like phenological similarity. When the 31 candidate unknown fields were compared with the maize reference trajectory, their DTW distances ranged from 0.151 to 0.565. Fourteen of the 31 candidate fields fell within the validation-distance range observed for confirmed maize fields, while 17 candidate fields had distances above this range. These results indicate that some candidate fields showed temporal behaviour similar to confirmed maize, whereas others showed weaker similarity and should therefore not be interpreted as confirmed maize fields.

### *3.2. DAP-Aligned Maize Phenology*

The DAP-aligned analysis showed that maize NDVI increased progressively after planting, reached peak greenness during the main vegetative growth period and then declined during crop maturity and senescence. Aligning observations by Days After Planting reduced the effect of different planting dates and allowed the maize growth pattern to be interpreted in relation to crop age rather than calendar date (Figure 4).

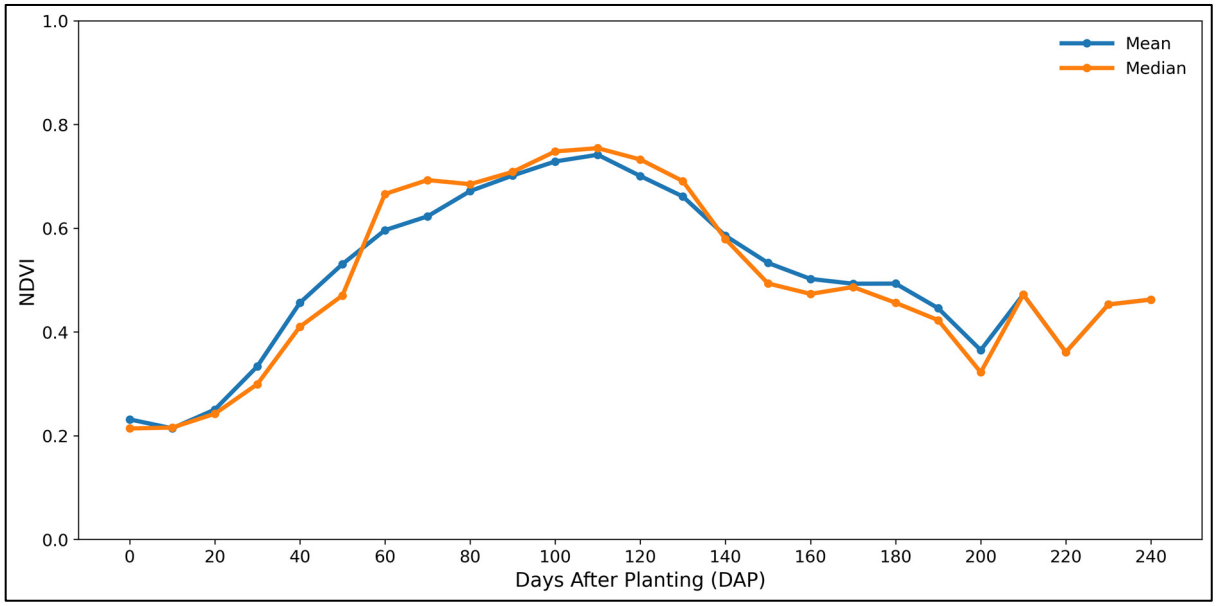



**Figure 4.** Mean and median NDVI trajectories of maize aligned by DAP.

Mean NDVI values were low during the early post-planting period, with values of approximately 0.22 during the first 10 days after planting. NDVI then increased steadily as the maize canopy developed, reaching its highest values between approximately 90 and 120 DAP. Thereafter, NDVI declined as the crop matured and senesced. The strongest

observation support occurred during the main growth period, while later DAP intervals had fewer observations and should therefore be interpreted more cautiously (Supplementary Figure S1). The DAP analysis was most useful for interpreting maize growth dynamics rather than for improving multi-crop classification, because later multi-crop experiments showed that calendar-date information remained important for discriminating annual crops.

### *3.3. Multi-Crop Reference Trajectories*

The crop-specific reference trajectories showed distinct seasonal NDVI behaviour among maize, soybean, potato and tea. Tea maintained relatively high NDVI values throughout the analysis period, reflecting its perennial canopy structure. In contrast, maize, soybean and potato showed more seasonal NDVI profiles, with clearer periods of establishment, canopy development, peak greenness and decline (Figure 5).

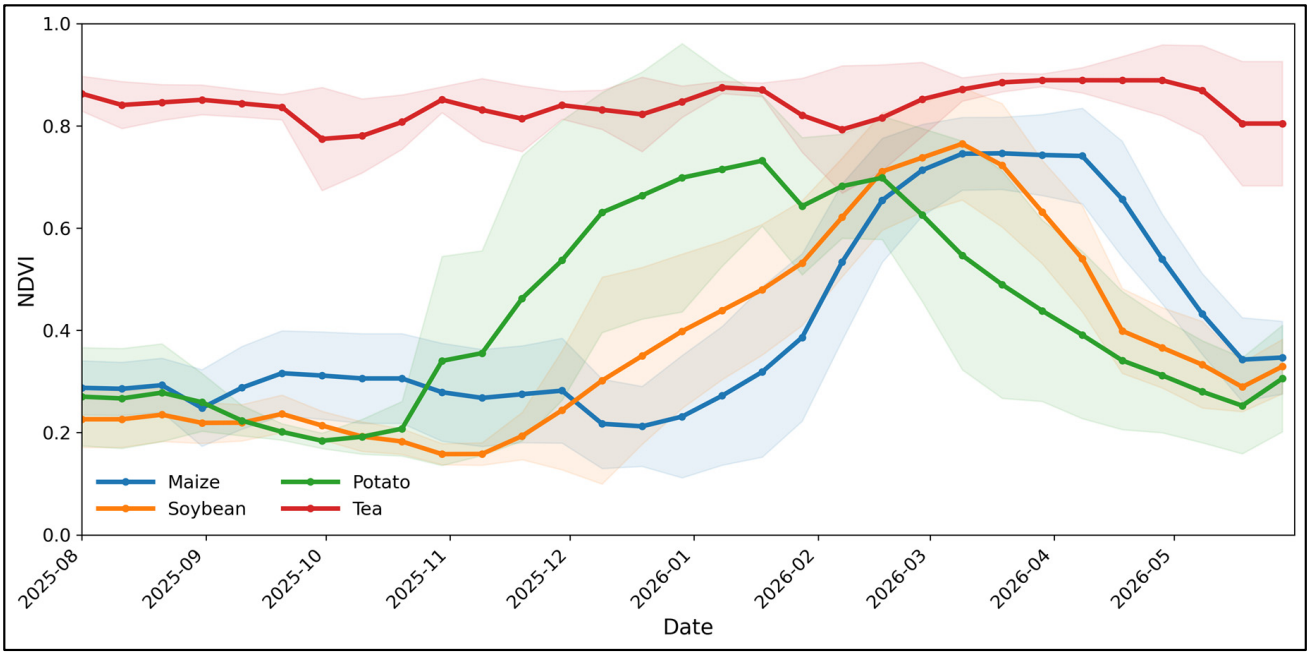



**Figure 5.** Calendar-date Sentinel-2 NDVI reference trajectories for maize, soybean, potato and tea. Shaded areas represent ±1 standard deviation around the class mean.

The reference trajectories showed that calendar-date timing contributed to crop separability. Although maize, soybean and potato all showed seasonal growth patterns, their NDVI increases, peaks and declines occurred at different times during the growing season. These differences provided useful temporal information for field-boundary classification.

### *3.4. Multi-Crop Classification Accuracy*

#### 3.4.1. Simple Mean-Reference DTW Baseline

The initial mean-reference DTW classifier achieved an overall accuracy of 80.0% on the 70 independent validation fields. Balanced accuracy was 75.5%, Cohen's kappa was 0.714, macro-F1 was 75.8% and weighted-F1 was 79.5%. Tea was classified most reliably, with all 16 validation tea fields correctly classified. Maize also showed strong performance, with 25 of 30 validation fields correctly classified. Soybean achieved moderate performance, with 11 of 14 validation fields correctly classified. Potato was the weakest class, with only four of 10 validation fields correctly classified. Most potato errors involved confusion with soybean and maize, indicating overlap in annual-crop NDVI trajectories (Tables 4 and 5).

**Table 4.** Confusion matrix for the simple mean-reference DTW baseline.

| Observed | Predicted | | | | |
|---|---|---|---|---|---|
| | **Maize** | **Potato** | **Soybean** | **Tea** | **Total** |
| Maize | 25 | 1 | 4 | 0 | 30 |
| Potato | 2 | 4 | 4 | 0 | 10 |
| Soybean | 3 | 0 | 11 | 0 | 14 |
| Tea | 0 | 0 | 0 | 16 | 16 |
| Total | 30 | 5 | 19 | 16 | 70 |

**Table 5.** Class-level performance of the simple mean-reference DTW baseline.

| Class | Precision (%) | Recall (%) | F1-Score (%) | Support |
|---|---|---|---|---|
| Maize | 83.3 | 83.3 | 83.3 | 30 |
| Potato | 80.0 | 40.0 | 53.3 | 10 |
| Soybean | 57.9 | 78.6 | 66.7 | 14 |
| Tea | 100.0 | 100.0 | 100.0 | 16 |
| Overall accuracy | | | 80.0 | 70 |
| Macro average | 80.3 | 75.5 | 75.8 | 70 |
| Weighted average | 82.1 | 80.0 | 79.5 | 70 |

#### 3.4.2. DTW Sensitivity Testing and CV-Selected DTW-kNN

DTW sensitivity testing showed that classification performance improved substantially when individual reference-field trajectories, rather than a single mean trajectory per crop class, were used as the comparison basis for classification. Training-only five-fold cross-validation within the 144 reference fields selected DTW-kNN with k = 1 and a one-composite warping window as the final DTW-based classifier. This configuration achieved a mean cross-validated accuracy of 93.1%, balanced accuracy of 90.3%, macro-F1 of 90.9% and weighted-F1 of 92.9% within the reference data (Table 6).

**Table 6.** Training-only cross-validation results for DTW-kNN parameter selection.

| k | Warping Window | Accuracy (%) | Balanced Accuracy (%) | Macro-F1 (%) | Weighted-F1 (%) |
|---|---|---|---|---|---|
| 1 | 1 | 93.1 | 90.3 | 90.9 | 92.9 |
| 1 | 2 | 91.6 | 89.5 | 89.5 | 91.5 |
| 3 | 1 | 91.0 | 88.0 | 88.2 | 90.9 |
| 3 | 2 | 88.2 | 88.1 | 87.2 | 88.5 |
| 1 | 3 | 88.9 | 86.2 | 86.8 | 88.6 |
| 1 | 4 | 88.8 | 86.2 | 86.7 | 88.6 |

When evaluated on the 70 independent validation fields, the selected DTW-kNN classifier achieved an overall accuracy of 92.9%, a balanced accuracy of 93.9%, a Cohen's kappa of 0.899, a macro-F1 of 93.6% and a weighted-F1 of 92.9%. This represented a substantial improvement over the initial mean-reference DTW baseline, which achieved 80.0% accuracy. The selected DTW-kNN classifier correctly classified 65 of the 70 validation fields. Potato and tea were perfectly classified, with 10 of 10 potato fields and 16 of 16 tea fields correctly predicted (Table 7).

**Table 7.** Confusion matrix for the selected DTW-kNN classifier.

| Observed | Predicted | | | | |
|---|---|---|---|---|---|
| | **Maize** | **Potato** | **Soybean** | **Tea** | **Total** |
| Maize | 27 | 0 | 3 | 0 | 30 |
| Potato | 0 | 10 | 0 | 0 | 10 |
| Soybean | 2 | 0 | 12 | 0 | 14 |
| Tea | 0 | 0 | 0 | 16 | 16 |
| Total | 29 | 10 | 15 | 16 | 70 |

Maize achieved 90.0% recall, with 27 of 30 fields correctly classified, while soybean achieved 85.7% recall, with 12 of 14 fields correctly classified. The remaining errors occurred only between maize and soybean, with three maize fields classified as soybean and two soybean fields classified as maize (Tables 7 and 8).

**Table 8.** Class-level performance of the selected DTW-kNN classifier.

| Class | Precision (%) | Recall (%) | F1-Score (%) | Support |
|---|---|---|---|---|
| Maize | 93.1 | 90.0 | 91.5 | 30 |
| Potato | 100.0 | 100.0 | 100.0 | 10 |
| Soybean | 80.0 | 85.7 | 82.8 | 14 |
| Tea | 100.0 | 100.0 | 100.0 | 16 |
| Overall accuracy | | | 92.9 | 70 |
| Macro average | 93.3 | 93.9 | 93.6 | 70 |
| Weighted average | 93.1 | 92.9 | 92.9 | 70 |

These results indicate that the main limitation of the initial DTW approach was not DTW itself, but the use of a single mean reference trajectory per crop. The DTW-kNN approach retained individual reference-field variability and allowed each validation field to match the most similar known crop trajectory.

#### 3.4.3. Comparison of Classifier Performance

The machine-learning benchmark models also performed strongly on the independent validation dataset. Random Forest and Support Vector Machine produced the highest validation accuracies, each achieving 95.7% overall accuracy and Cohen's kappa of 0.939. Distance-weighted k-nearest neighbour achieved 94.3% accuracy, while Ridge Classifier achieved 91.4%. The selected DTW-kNN classifier achieved 92.9% accuracy, placing it above Ridge Classifier but slightly below distance-weighted kNN, Random Forest and Support Vector Machine. The benchmark comparison shows that conventional machine-learning models provided the highest overall accuracies, but the selected DTW-kNN classifier was competitive. Unlike the feature-space machine-learning models, the DTW-kNN classifier retained a direct temporal-similarity interpretation, because each prediction was based on similarity to known crop NDVI trajectories (Table 9).

### *3.5. Prediction of Unknown Fields Using the Selected DTW-kNN Classifier*

The selected DTW-kNN classifier was applied to the 128 unknown field polygons to produce field-level crop predictions. Because these fields had no confirmed crop labels, the results were interpreted as predictions rather than independent accuracy-assessment outputs. Of the 128 unknown fields, 106 were predicted as maize, representing 82.8% of the unknown-field dataset. The remaining 22 fields were predicted as soybean, representing

17.2%. No unknown fields were predicted as potato or tea by the selected DTW-kNN classifier (Table 10).

**Table 9.** Comparison of DTW-based and machine-learning classifiers.

| Method | Overall Accuracy (%) | Balanced Accuracy (%) | Cohen's Kappa | Macro-F1 (%) | Weighted-F1 (%) |
|---|---|---|---|---|---|
| Mean-reference DTW, no window | 80.0 | 75.5 | 0.714 | 75.8 | 79.5 |
| CV-selected DTW-kNN, (k = 1, window = 1) | 92.9 | 93.9 | 0.899 | 93.6 | 92.9 |
| Ridge | 91.4 | 94.0 | 0.880 | 92.5 | 91.5 |
| DW-kNN | 94.3 | 94.0 | 0.919 | 94.1 | 94.4 |
| RF | 95.7 | 95.6 | 0.939 | 96.0 | 95.7 |
| SVM | 95.7 | 94.9 | 0.939 | 95.3 | 95.8 |

**Table 10.** Unknown-field predictions by DTW confidence category.

| Predicted Class | High Confidence | Moderate Confidence | Low Confidence | Total | Percentage (%) |
|---|---|---|---|---|---|
| Maize | 79 | 15 | 12 | 106 | 82.8 |
| Soybean | 5 | 6 | 11 | 22 | 17.2 |
| Total | 84 | 21 | 23 | 128 | 100.0 |

Most unknown-field predictions had high DTW confidence. Overall, 84 fields, or 65.6%, were assigned to the high-confidence category, 21 fields, or 16.4%, were assigned to the moderate-confidence category, and 23 fields, or 18.0%, were classified as low or uncertain confidence. Among fields predicted as maize, 79 were high confidence, 15 were moderate confidence and 12 were low or uncertain. Among fields predicted as soybean, five were high confidence, six were moderate confidence and 11 were low or uncertain. The confidence results indicate that most maize predictions were clearly separated from the next-best crop class, while soybean predictions were more uncertain. This uncertainty is consistent with the remaining validation errors, which occurred only between maize and soybean. The spatial distribution of the predicted crop classes is shown in Figure 6, while the DTW confidence classes are provided in Supplementary Figure S2.

### *3.6. Effect of DAP Alignment on Multi-Crop Classification*

The DAP alignment experiment showed that crop-age alignment was useful for interpreting maize phenology but did not improve multi-crop classification. When DAP-based DTW classification was applied to maize, soybean and potato fields with known planting dates, the full DAP-DTW approach achieved 49.1% accuracy. Restricting the analysis to the 0–160 DAP period further reduced accuracy to 32.1%. These results indicate that DAP alignment removed useful calendar-date information that helped distinguish annual crops in the multi-crop classification task. Although aligning by Days After Planting improved the biological interpretation of maize growth, calendar-date trajectories were more informative for separating crop types at field-boundary scale in this dataset.

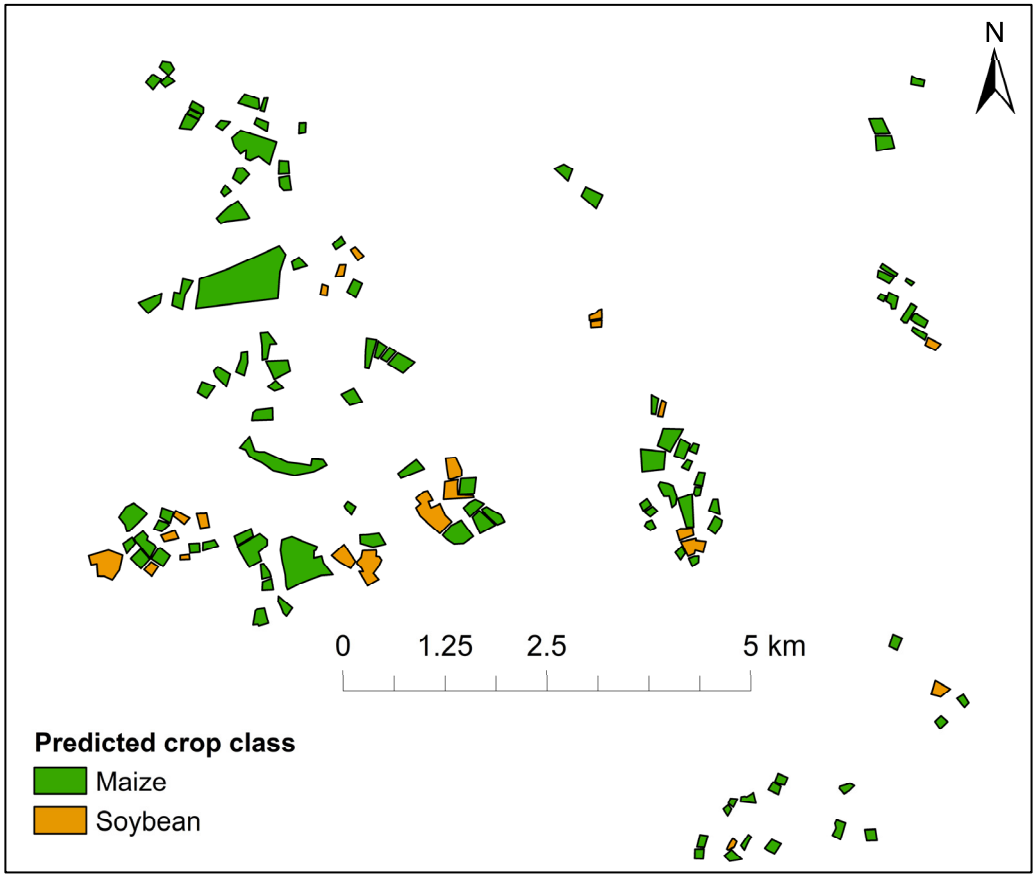



**Figure 6.** Spatial distribution of DTW-kNN predicted crop class for the unknown fields.

## 4. Discussion

### *4.1. Sentinel-2 NDVI Time Series Captured Crop-Specific Temporal Behaviour*

The results demonstrate that Sentinel-2 NDVI time series captured meaningful differences in crop seasonal development at field-boundary scale, with the maize reference trajectory showing a clear pattern of establishment, canopy development, peak greenness and senescence. This confirms that even in heterogeneous smallholder landscapes, where planting dates, cultivars and management practices vary among fields, maize fields can still exhibit a recognisable seasonal NDVI signal when analysed as temporal trajectories rather than as single-date observations. This is consistent with previous work done in other regions and cropping systems, which showed that NDVI time series can capture crop establishment, canopy development, peak greenness and senescence in agricultural landscapes [23–26,76,77].

The DAP-aligned analysis further supported this interpretation. By converting calendar-date observations into DAP, the analysis showed that maize NDVI increased after planting, reached peak greenness between approximately 90 and 120 DAP, and declined thereafter. This crop-age alignment helped describe maize phenological behaviour more directly than calendar-date alignment because it reduced the effect of different planting dates among farms. Similar patterns have been reported when maize or corn NDVI is expressed on a DAP axis.

For example, Tamás et al. [76] reported maximum UAV-derived maize NDVI around 90 DAP under experimental conditions, while Venancio et al. [75] showed that OLI- and MODIS-derived NDVI followed a rapid increase, intermediate stabilisation and late-season decline across corn phenological stages. Manimozhian and Chandel [77] also showed the value of organising Sentinel-2 observations according to DAP-defined growth-stage

windows to improve phenological interpretation across seasons with variable planting dates. In the present study, DAP alignment should therefore be interpreted mainly as an agronomic and phenological interpretation step. It helped describe maize growth dynamics in a smallholder setting with staggered planting dates, although calendar-date information remained more useful for separating multiple crop types.

The multi-crop reference trajectories also showed that crop type influenced the shape and timing of NDVI development. Tea was clearly separable because of its perennial canopy and consistently high NDVI values, whereas maize, soybean and potato showed more seasonal trajectories. Distinguishing perennial tea from annual crops was not the main challenge; rather, the difficulty lay in separating annual crops whose canopy development partly overlapped during the growing season.

### *4.2. Mean-Reference DTW Was Interpretable but Limited*

The initial mean-reference DTW classifier achieved 80.0% accuracy on the independent validation dataset. However, the class-level results also showed that the mean-reference approach had important limitations, especially for potato and soybean.

The main limitation of the mean-reference approach was its representation of each crop using only one average temporal trajectory. In smallholder farming systems, crop fields belonging to the same class may differ in planting date, cultivar, irrigation status, fertiliser use, crop condition, weed pressure and harvesting stage. Similar concerns have been raised in DTW-based crop-mapping studies, where differences in crop calendars, planting management and phenological timing can affect temporal similarity matching and motivate the use of time-weighted or constrained DTW approaches [29,43]. Averaging smallholder fields into a single reference curve can suppress important within-class variability. As a result, validation fields that are genuine examples of a crop may appear less similar to the crop mean than to another crop's mean trajectory.

This explains why the original mean-reference DTW approach performed reasonably well for maize and tea, but less well for potato and soybean. Tea fields had a distinct perennial NDVI pattern, making them easier to classify. Maize also had a relatively strong seasonal signal. Potato and soybean, however, were more vulnerable to confusion because their seasonal NDVI curves overlapped with other annual crops during parts of the growing season.

### *4.3. DTW-kNN Improved Classification by Preserving Reference-Field Variability*

The DTW-kNN results show that DTW performance improved substantially when individual reference-field trajectories were retained instead of being averaged into a single crop mean. After training-only cross-validation across candidate k and window values, the best-performing DTW-kNN configuration used k = 1 and a one-composite warping window. When applied to the independent validation fields, this model achieved 92.9% overall accuracy, compared with the 80.0% achieved by the original mean-reference DTW classifier.

Previous DTW-based crop-mapping studies have mainly improved temporal matching through time-weighted or time-constrained formulations, object-based mapping, SAR time series, or limited-sample strategies. For example, Belgiu and Csillik [43] evaluated pixel- and object-based time-weighted DTW for Sentinel-2 cropland mapping, while Csillik et al. [47] developed an object-based time-constrained DTW workflow using Sentinel-2 vegetation index time series. Gella et al. [45] demonstrated that DTW and SAR imagery can support crop-type mapping in fragmented landscapes with small farm plots, and Xiao et al. [29] tested time-weighted DTW under limited-sample conditions using Sentinel-1 and GEE. In contrast to these studies, the present study shows that a simple but important

modification, retaining individual reference-field trajectories and implementing DTW as a kNN classifier, improved classification in this dataset while preserving the interpretability of trajectory-based matching.

This improvement indicates that the main weakness was not DTW itself, but the way the reference trajectories were represented. The DTW-kNN approach allowed each validation field to be matched to the most similar individual reference field. This is particularly important in smallholder landscapes because fields of the same crop may not follow exactly the same NDVI curve. By retaining field-level variability, DTW-kNN provided a more flexible crop-matching approach while still preserving the temporal-similarity logic of DTW.

The constrained warping window also improved the biological realism of the DTW comparison. Unconstrained DTW can allow excessive temporal shifting, which may align unrelated crop stages and produce misleading similarity scores. The selected one-composite window allowed limited flexibility in crop timing while preventing unrealistic matching between very different parts of the growing season. This is important in agricultural applications because temporal flexibility is useful, but crop growth stages should not be allowed to shift without constraint.

The DTW-kNN classifier correctly classified all potato and tea validation fields and reduced the remaining errors to maize–soybean confusion. This result suggests that the improved DTW design was able to capture more of the crop-specific temporal structure than the simple mean-reference approach. However, the remaining maize–soybean confusion shows that some annual crop trajectories remained similar, especially where their growth periods and canopy development overlapped.

### *4.4. Implications of Benchmark Classifier Comparison*

The benchmark comparison showed that conventional machine-learning models achieved the highest overall accuracies. RF and SVM each achieved 95.7% accuracy, followed by distance-weighted kNN at 94.3%. The selected DTW-kNN classifier achieved 92.9%, while Ridge Classifier achieved 91.4%. The strong performance of RF and SVM was not unexpected, as these classifiers are widely reported in crop-mapping and multi-temporal satellite-image classification literature as effective conventional machine-learning approaches when multi-temporal spectral features are available [1,10,20,30–32].

Although RF and SVM produced the highest accuracies, the selected DTW-kNN classifier remained competitive. Its advantage is interpretability. RF, SVM and distance-weighted kNN classify fields using patterns across the full set of NDVI time-step features, whereas DTW-kNN classifies fields by directly comparing the shape and timing of observed crop trajectories with known reference-field trajectories. This makes the DTW-kNN classification logic easier to explain in phenological terms. The distinction is important in smallholder crop-monitoring applications, where limited reference data, variable crop calendars and the need for transparent outputs can influence method selection [1,20,42].

These results suggest that DTW and machine learning can serve different purposes. If the main goal is maximum classification accuracy, RF or SVM may be preferable. If the goal is interpretable temporal matching, crop phenology assessment and transparent field-level comparison with known crop trajectories, DTW-kNN provides an alternative. In this study, the improved DTW-kNN approach narrowed the performance gap between DTW and conventional machine-learning classifiers while retaining the interpretability of trajectory-based classification.

### *4.5. DAP Alignment Improved Maize Interpretation but Not Multi-Crop Classification*

The DAP-aligned maize analysis was useful for describing maize phenology, but it did not improve multi-crop classification. Although aligning observations by DAP reduced the

effect of different planting dates and helped describe maize growth in relation to crop age, the DAP-based multi-crop DTW results were weaker than the calendar-date approach. This indicates that calendar timing contained useful information for separating crop types in this dataset.

This finding highlights an important distinction between phenological interpretation and crop classification. DAP alignment is useful when the objective is to understand maize development after planting, but calendar-date trajectories were more informative for distinguishing maize, soybean, potato and tea. Similar multi-temporal crop-classification studies have shown that both phenological shape and seasonal timing can contribute to crop separability [18,23,24,41].

### *4.6. Operational Relevance and Limitations for Smallholder Crop Mapping*

The selected DTW-kNN classifier was applied to 128 unknown field polygons to demonstrate its operational use in an unlabelled cultivated area. Most unknown fields were predicted as maize, while a smaller proportion were predicted as soybean. Most predictions were also assigned to the high-confidence category, indicating clear separation between the closest and second-closest crop classes for many fields.

However, these unknown-field outputs should be interpreted as predictions rather than confirmed crop labels. The unknown fields had no independent ground-truth observations, so they could not be used for accuracy assessment. The confidence classes provide a useful indication of DTW separation, but they are not calibrated probabilities. They should therefore be used as practical indicators of classification certainty rather than definitive measures of prediction reliability.

The study also remains limited by the availability and distribution of field-reference data. The validation dataset was independent, but it was still relatively small, particularly for potato and soybean. In addition, the analysis was conducted within one growing season and one smallholder landscape. Further testing across additional seasons, districts and crop mixtures would be needed to evaluate temporal and spatial transferability. Field-boundary quality is another important limitation because all analyses were conducted at the polygon level. Errors in field delineation, mixed fields, boundary overlap or within-field crop heterogeneity could affect extracted NDVI trajectories and classification results.

Another limitation is that the analysis was based only on Sentinel-2 NDVI. NDVI is useful for describing canopy greenness and seasonal phenological development, but it may not fully capture differences in crop structure, chlorophyll status, soil background or canopy architecture. This may partly explain the remaining confusion between maize and soybean. Future work should therefore evaluate whether additional Sentinel-2 indices, including EVI, red-edge indices such as NDRE, and moisture-sensitive indices such as NDWI or NDMI, can improve the separation of annual crops that have similar NDVI trajectories. Sentinel-1 SAR data should also be tested because radar observations are less affected by cloud cover and may provide complementary structural information. In addition, future operational applications should consider automated field-boundary extraction and pixel-level or wall-to-wall mapping approaches where complete field-boundary layers are unavailable.

At the field-boundary scale used in this study, DTW computation was manageable because the analysis involved 144 reference fields, 70 validation fields, 128 prediction fields and 31 ten-day NDVI time steps. However, for larger operational applications, computational demand would increase with the number of field polygons, reference trajectories and time steps, and would therefore require efficient implementation, parallel processing or candidate filtering.

Despite the limitations, the results show that Sentinel-2 NDVI time series combined with DTW-kNN can provide an interpretable and effective approach for field-scale crop

classification in smallholder systems. The method is particularly useful where crop calendars are variable, fields are fragmented, and transparent trajectory-based classification is desirable.

## 5. Conclusions

This study evaluated Sentinel-2 NDVI time series and DTW-based approaches, including DTW-kNN, for field-scale maize identification and multi-crop classification in a heterogeneous smallholder farming landscape. The results showed that maize fields followed a recognisable seasonal NDVI trajectory despite differences in planting dates, cultivars and management conditions. The DAP-aligned analysis further confirmed that maize NDVI increased after planting, reached peak greenness between approximately 90 and 120 DAP, and declined during maturity and senescence.

For multi-crop classification, the initial mean-reference DTW approach achieved 80.0% accuracy, demonstrating that crop-specific NDVI temporal trajectories contain useful classification information. However, performance improved substantially when individual reference-field trajectories were retained using DTW-kNN. The CV-selected DTW-kNN configuration achieved 92.9% accuracy on the independent validation dataset, indicating that within-class variability is important in smallholder crop-classification problems. The remaining errors were limited to confusion between maize and soybean, while potato and tea were correctly classified in the validation dataset.

The benchmark comparison showed that RF and SVM achieved the highest overall accuracies, each reaching 95.7%. Nevertheless, the selected DTW-kNN classifier was competitive with these machine-learning models while retaining a more direct temporal-similarity interpretation. This suggests that DTW-kNN provides a useful balance between classification performance and interpretability, particularly where the objective is to relate field-level predictions to known crop phenological trajectories.

When applied to unknown field polygons, the selected DTW-kNN classifier predicted most fields as maize, with a smaller proportion predicted as soybean. These predictions demonstrate the potential operational use of Sentinel-2 time-series classification for smallholder crop mapping. However, because the unknown fields had no confirmed crop labels, these outputs should be treated as predictions rather than independently validated crop classes. Future work should expand the reference and validation datasets across additional seasons, districts and crop mixtures, test complementary Sentinel-2 vegetation indices and Sentinel-1 SAR data, and evaluate the transferability of DTW-kNN and machine-learning classifiers under different smallholder farming conditions. Further work should also assess automated field-boundary extraction and pixel-level or wall-to-wall classification approaches for areas where complete field-boundary datasets are not available.

**Supplementary Materials:** The following supporting information can be downloaded at https://www.mdpi.com/article/10.3390/app162111065/s1, Figure S1: Observation support across DAP intervals for the maize phenology analysis; Figure S2: Spatial distribution of DTW confidence classes for the unknown fields classified using the selected DTW-kNN model.

**Author Contributions:** Conceptualization: W.M., P.W.K. and J.G.C.; Data curation: W.M.; Formal analysis: W.M.; Funding acquisition: W.M., P.W.K. and J.G.C.; Investigation: W.M. and P.W.K.; Methodology: W.M. and P.W.K.; Project administration: W.M., J.G.C. and P.W.K.; Validation: J.G.C. and P.W.K.; Writing—original draft: W.M.; Writing—review and editing: J.G.C. and P.W.K. All authors have read and agreed to the published version of the manuscript.

**Funding:** This work was supported by the National Earth Observation and Space Secretariat (NEOSS) under the Agricultural Research Council's project number: ISC012601000001.

**Data Availability Statement:** The satellite data used in this study are publicly available. Shapefiles and farm boundaries are available upon reasonable request through the first author.

**Acknowledgments:** The authors wish to thank South Africa's Agricultural Research Council (ARC) for supporting this work and the National Earth Observation and Space Secretariat (NEOSS) for funding the research activities that enabled the writing of this paper. We thank Lulekwa Makapela, Christelle Taylor, and Kwanele Ngongoma for project coordination. We also thank farmers and officials from the Eastern Cape's Department of Agriculture for providing cropping information.

**Conflicts of Interest:** Author Pitso Walter Khoboko was employed by Neria Solutions. The remaining authors declare that the research was conducted in the absence of any commercial or financial relationships that could be construed as a potential conflict of interest.

## Abbreviations

The following abbreviations are used in this manuscript:

| | |
|---|---|
| DAP | Days After Planting |
| DTW | Dynamic Time Warping |
| DTW-kNN | Dynamic Time Warping k-nearest neighbour |
| GEE | Google Earth Engine |
| kNN | k-nearest neighbour |
| NDVI | Normalised Difference Vegetation Index |
| ORTDM | O.R. Tambo District Municipality |
| RF | Random Forest |
| SAR | Synthetic Aperture Radar |
| SVM | Support Vector Machine |
| UAV | Unmanned Aerial Vehicle |

## References

1. Khosravi, I. Advancements in Crop Mapping through Remote Sensing: A Comprehensive Review of Concept, Data Sources, and Procedures over Four Decades. *Remote Sens. Appl.* **2025**, *38*, 101527. [CrossRef]
2. Mathenge, M.; Sonneveld, B.G.J.S.; Broerse, J.E.W. Application of GIS in Agriculture in Promoting Evidence-Informed Decision Making for Improving Agriculture Sustainability: A Systematic Review. *Sustainability* **2022**, *14*, 9974. [CrossRef]
3. You, L.; Sun, Z. Mapping Global Cropping System: Challenges, Opportunities, and Future Perspectives. *Crop Environ.* **2022**, *1*, 68–73. [CrossRef]
4. Orynbaikyzy, A.; Gessner, U.; Conrad, C. Crop Type Classification Using a Combination of Optical and Radar Remote Sensing Data: A Review. *Int. J. Remote Sens.* **2019**, *40*, 6553–6595. [CrossRef]
5. Mashaba-Munghemezulu, Z.; Chirima, G.J.; Munghemezulu, C. Mapping Smallholder Maize Farms Using Multi-Temporal Sentinel-1 Data in Support of the Sustainable Development Goals. *Remote Sens.* **2021**, *13*, 1666. [CrossRef]
6. Schmedtmann, J.; Campagnolo, M.L. Reliable Crop Identification with Satellite Imagery in the Context of Common Agriculture Policy Subsidy Control. *Remote Sens.* **2015**, *7*, 9325–9346. [CrossRef]
7. Tang, F.H.M.; Nguyen, T.H.; Conchedda, G.; Casse, L.; Tubiello, F.N.; Maggi, F. CROPGRIDS: A Global Geo-Referenced Dataset of 173 Crops. *Sci. Data* **2024**, *11*, 413. [CrossRef] [PubMed]
8. Tsiligiridis, T.; Ainali, K. Remote Sensing Big AgriData for Food Availability. In Proceedings of the 2018 International Conference on Image and Video Processing, and Artificial Intelligence, Shanghai, China, 15–17 August 2018. [CrossRef]
9. Choukri, M.; Laamrani, A.; Chehbouni, A. Use of Optical and Radar Imagery for Crop Type Classification in Africa: A Review. *Sensors* **2024**, *24*, 3618. [CrossRef] [PubMed]
10. Farooq, A.; Farooq, N.; Akbar, H.; Hassan, Z.U.; Gheewala, S.H. A Critical Review of Climate Change Impact at a Global Scale on Cereal Crop Production. *Agronomy* **2023**, *13*, 162. [CrossRef]
11. Debats, S.R.; Luo, D.; Estes, L.D.; Fuchs, T.J.; Caylor, K. A Generalized Computer Vision Approach to Mapping Crop Fields in Heterogeneous Agricultural Landscapes. *Remote Sens. Environ.* **2016**, *179*, 210–221. [CrossRef]
12. Masiza, W.; Chirima, J.; Hamandawana, H.; Pillay, R. Enhanced Mapping of a Smallholder Crop Farming Landscape through Image Fusion and Model Stacking. *Int. J. Remote Sens.* **2020**, *41*, 8739–8756. [CrossRef]
13. Sidike, P.; Sagan, V.; Maimaitijiang, M.; Maimaitiyiming, M.; Shakoor, N.; Burken, J.; Mockler, T.; Fritschi, F.B. DPEN: Deep Progressively Expanded Network for Mapping Heterogeneous Agricultural Landscape Using WorldView-3 Satellite Imagery. *Remote Sens. Environ.* **2019**, *221*, 756–772. [CrossRef]

14. Black, E.; Asfaw, D.T.; Sananka, A.; Aston, S.; Boult, V.L.; Maidment, R.I. Application of TAMSAT-ALERT Soil Moisture Forecasts for Planting Date Decision Support in Africa. *Front. Clim.* **2023**, *4*, 993511. [CrossRef]
15. Masiza, W.; Nkuna, B.L.; Ratshiedana, P.E.; Madasa, A.; Nduku, L.; Shwatja, T.; Chirima, J.G.; Nyamugama, A.; Abutaleb, K.; Khoboko, P.W.; et al. Predicting Smallholder Maize Yield Using Sentinel-2-Derived Phenological Metrics. *Smart Agric. Technol.* **2026**, *13*, 101870. [CrossRef]
16. Prudente, V.H.R.; Garcia-Medina, M.; Krishna, V.; Euler, M.; Bhattarai, N.; Lerner, A.M.; McDonald, A.J.; Sherpa, S.; Rajan, H.; Urfels, A.; et al. Mapping Grain Crop Sowing Date in Smallholder Systems Using Optical Imagery. *Remote Sens. Appl.* **2025**, *39*, 101660. [CrossRef]
17. Whitcraft, A.K.; Vermote, E.F.; Becker-Reshef, I.; Justice, C.O. Cloud Cover throughout the Agricultural Growing Season: Impacts on Passive Optical Earth Observations. *Remote Sens. Environ.* **2015**, *156*, 438–447. [CrossRef]
18. Pluto-Kossakowska, J. Review on Multitemporal Classification Methods of Satellite Images for Crop and Arable Land Recognition. *Agriculture* **2021**, *11*, 999. [CrossRef]
19. Keogh, E.J.; Pazzani, M.J. Derivative Dynamic Time Warping. In Proceedings of the 2001 SIAM International Conference on Data Mining (SDM), Chicago, IL, USA, 5–7 April 2001. [CrossRef]
20. Qiu, L.; Qiu, C.; Song, C. ESDTW: Extrema-Based Shape Dynamic Time Warping. *Expert Syst. Appl.* **2024**, *239*, 122432. [CrossRef]
21. Huang, S.; Tang, L.; Hupy, J.P.; Wang, Y.; Shao, G. A Commentary Review on the Use of Normalized Difference Vegetation Index (NDVI) in the Era of Popular Remote Sensing. *J. For. Res.* **2021**, *32*, 1–6. Correction in *J. For. Res.* **2021**, *32*, 2719. https://doi.org/10.1007/s11676-020-01155-1. [CrossRef]
22. Rouse, J.; Haas, R.; Schell, J.; Deering, D. Monitoring Vegetation Systems in the Great Plains with ERTS. In Proceedings of the Third ERTS-1 Symposium, NASA SP-351, Washington, DC, USA, 10–14 December 1973.
23. Pan, Z.; Huang, J.; Zhou, Q.; Wang, L.; Cheng, Y.; Zhang, H.; Blackburn, G.A.; Yan, J.; Liu, J. Mapping Crop Phenology Using NDVI Time-Series Derived from HJ-1 A/B Data. *Int. J. Appl. Earth Obs. Geoinf.* **2015**, *34*, 188–197. [CrossRef]
24. Seo, B.; Lee, J.; Lee, K.D.; Hong, S.; Kang, S. Improving Remotely-Sensed Crop Monitoring by NDVI-Based Crop Phenology Estimators for Corn and Soybeans in Iowa and Illinois, USA. *Field Crops Res.* **2019**, *238*, 113–128. [CrossRef]
25. Hu, J.; Liu, Z.; Luo, Z.; Ma, H.; Chen, P.; Song, Q.; Xu, B.; Zhan, Y.; Cai, Z. Mapping Diverse Rice Cropping Patterns with Limited Samples by Learning Phenology-Aligned Temporal Similarity from Multi-Source Remote Sensing Data. *J. Integr. Agric.* **2026**, *in press*. [CrossRef]
26. Salas, E.A.L.; Subburayalu, S.K.; Slater, B.; Zhao, K.; Bhattacharya, B.; Tripathy, R.; Das, A.; Nigam, R.; Dave, R.; Parekh, P. Mapping Crop Types in Fragmented Arable Landscapes Using AVIRIS-NG Imagery and Limited Field Data. *Int. J. Image Data Fusion* **2019**, *11*, 33–56. [CrossRef]
27. Xiao, X.; Jiang, L.; Liu, Y.; Ren, G. Limited-Samples-Based Crop Classification Using a Time-Weighted Dynamic Time Warping Method, Sentinel-1 Imagery, and Google Earth Engine. *Remote Sens.* **2023**, *15*, 1112. [CrossRef]
28. Shao, Y.; Ren, J.; Campbell, J.B. Multitemporal Remote Sensing Data Analysis for Agricultural Application. In *Comprehensive Remote Sensing*; Elsevier: Amsterdam, The Netherlands, 2018; Volume 9, pp. 29–38. [CrossRef]
29. Alami Machichi, M.; Mansouri, L.E.; Imani, Y.; Bourja, O.; Lahlou, O.; Zennayi, Y.; Bourzeix, F.; Hanadé Houmma, I.; Hadria, R. Crop Mapping Using Supervised Machine Learning and Deep Learning: A Systematic Literature Review. *Int. J. Remote Sens.* **2023**, *44*, 2717–2753. [CrossRef]
30. Wu, F.; Maleki, R.; Oubara, A.; Gómez, D.; Eftekhari, A.; Yang, G. Machine Learning Approaches for Crop Identification from Remote Sensing Imagery: A Review. In *Proceedings of the 14th International Conference on Soft Computing and Pattern Recognition (SoCPaR 2022)*; Lecture Notes in Networks and Systems (LNNS); Springer: Cham, Switzerland, 2023; Volume 648. [CrossRef]
31. Cheng, X.; Sun, Y.; Zhang, W.; Wang, Y.; Cao, X.; Wang, Y. Application of Deep Learning in Multitemporal Remote Sensing Image Classification. *Remote Sens.* **2023**, *15*, 3859. [CrossRef]
32. da Silva, M.P.; Correa, S.P.L.P.; Schaefer, M.A.R.; Reis, J.C.S.; Nunes, I.M.; dos Santos, J.A.; Oliveira, H.N. Advancing Agricultural Remote Sensing: A Comprehensive Review of Deep Supervised and Self-Supervised Learning for Crop Monitoring. *Comput. Graph.* **2025**, *133*, 104434. [CrossRef]
33. Joshi, A.; Pradhan, B.; Gite, S.; Chakraborty, S. Remote-Sensing Data and Deep-Learning Techniques in Crop Mapping and Yield Prediction: A Systematic Review. *Remote Sens.* **2023**, *15*, 2014. [CrossRef]
34. Turkoglu, M.O.; D'Aronco, S.; Perich, G.; Liebisch, F.; Streit, C.; Schindler, K.; Wegner, J.D. Crop Mapping from Image Time Series: Deep Learning with Multi-Scale Label Hierarchies. *Remote Sens. Environ.* **2021**, *264*, 112603. [CrossRef]
35. Khan, H.R.; Gillani, Z.; Jamal, M.H.; Athar, A.; Chaudhry, M.T.; Chao, H.; He, Y.; Chen, M. Early Identification of Crop Type for Smallholder Farming Systems Using Deep Learning on Time-Series Sentinel-2 Imagery. *Sensors* **2023**, *23*, 1779. [CrossRef] [PubMed]
36. Khan, W.; Minallah, N.; Sher, M.; Khan, M.A.; Rehman, A.U.; Al-Ansari, T.; Bermak, A. Advancing Crop Classification in Smallholder Agriculture: A Multifaceted Approach Combining Frequency-Domain Image Co-Registration, Transformer-Based Parcel Segmentation, and Bi-LSTM for Crop Classification. *PLoS ONE* **2024**, *19*, e0299350. [CrossRef] [PubMed]

37. Waqas, M.; Naseem, A.; Humphries, U.W.; Hlaing, P.T.; Dechpichai, P.; Wangwongchai, A. Applications of Machine Learning and Deep Learning in Agriculture: A Comprehensive Review. *Green Technol. Sustain.* **2025**, *3*, 100199. [CrossRef]
38. Attri, I.; Awasthi, L.K.; Sharma, T.P.; Rathee, P. A Review of Deep Learning Techniques Used in Agriculture. *Ecol. Inform.* **2023**, *77*, 102217. [CrossRef]
39. Safonova, A.; Ghazaryan, G.; Stiller, S.; Main-Knorn, M.; Nendel, C.; Ryo, M. Ten Deep Learning Techniques to Address Small Data Problems with Remote Sensing. *Int. J. Appl. Earth Obs. Geoinf.* **2023**, *125*, 103569. [CrossRef]
40. Nakalembe, C.; Kerner, H. Considerations for AI-EO for Agriculture in Sub-Saharan Africa. *Environ. Res. Lett.* **2023**, *18*, 041002. [CrossRef]
41. Belgiu, M.; Csillik, O. Sentinel-2 Cropland Mapping Using Pixel-Based and Object-Based Time-Weighted Dynamic Time Warping Analysis. *Remote Sens. Environ.* **2018**, *204*, 509–523. [CrossRef]
42. Dong, Q.; Chen, X.; Chen, J.; Zhang, C.; Liu, L.; Cao, X.; Zang, Y.; Zhu, X.; Cui, X. Mapping Winter Wheat in North China Using Sentinel 2A/B Data: A Method Based on Phenology-Time Weighted Dynamic Time Warping. *Remote Sens.* **2020**, *12*, 1274. [CrossRef]
43. Gella, G.W.; Bijker, W.; Belgiu, M. Mapping Crop Types in Complex Farming Areas Using SAR Imagery with Dynamic Time Warping. *ISPRS J. Photogramm. Remote Sens.* **2021**, *175*, 171–183. [CrossRef]
44. Singh, R.K.; Rizvi, J.; Behera, M.D.; Biradar, C. Automated Crop Type Mapping Using Time-Weighted Dynamic Time Warping-A Basis to Derive Inputs for Enhanced Food and Nutritional Security. *Curr. Res. Environ. Sustain.* **2021**, *3*, 100032. [CrossRef]
45. Csillik, O.; Belgiu, M.; Asner, G.; Kelly, M. Object-Based Time-Constrained Dynamic Time Warping Classification of Crops Using Sentinel-2. *Remote Sens.* **2019**, *11*, 1257. [CrossRef]
46. Guo, Z.; Yang, K.; Liu, C.; Lu, X.; Cheng, L.; Li, M. Mapping National-Scale Croplands in Pakistan by Combining Dynamic Time Warping Algorithm and Density-Based Spatial Clustering of Applications with Noise. *Remote Sens.* **2020**, *12*, 3644. [CrossRef]
47. Li, H.Y.; Lawarence, J.A.; Mason, P.J.; Ghail, R.C. Fast Dynamic Time Warping and Hierarchical Clustering with Multispectral and Synthetic Aperture Radar Temporal Analysis for Unsupervised Winter Food Crop Mapping. *Agriculture* **2025**, *15*, 82. [CrossRef]
48. Rafif, R.; Kusuma, S.S.; Saringatin, S.; Nanda, G.I.; Wicaksono, P.; Arjasakusuma, S. Crop Intensity Mapping Using Dynamic Time Warping and Machine Learning from Multi-Temporal Planetscope Data. *Land* **2021**, *10*, 1384. [CrossRef]
49. Hajdu, F.; Neves, D.; Granlund, S. Changing Livelihoods in Rural Eastern Cape, South Africa (2002–2016): Diminishing Employment and Expanding Social Protection. *J. S. Afr. Stud.* **2020**, *46*, 743–772. [CrossRef]
50. Kepe, T. Magwa Tea Venture in South Africa: Politics, Land and Economics. *Soc. Dyn.* **2005**, *31*, 261–279. [CrossRef]
51. Mucina, L.; Rutherford, M.C. *The Vegetation of South Africa, Lesotho and Swaziland*; South African National Biodiversity Institute: Pretoria, South Africa, 2006.
52. Beck, H.E.; Zimmermann, N.E.; McVicar, T.R.; Vergopolan, N.; Berg, A.; Wood, E.F. Present and Future Köppen-Geiger Climate Classification Maps at 1-Km Resolution. *Sci. Data* **2018**, *5*, 180214. Correction in *Sci. Data* **2020**, *7*, 274. [CrossRef] [PubMed]
53. National Department of Agriculture. *Trends in the Agricultural Sector 2025*; National Department of Agriculture: Pretoria, South Africa, 2025. Available online: https://nda.gov.za/images/Branches/Economica%20Development%20Trade%20and%20Marketing/Statistc%20and%20%20Economic%20Analysis/statistical-information/trends-in-the-agricultural-sector-2025.pdf (accessed on 20 July 2026).
54. De Villiers, C.; Munghemezulu, C.; Tesfamichael, S.G.; Mashaba-Munghemezulu, Z.; Chirima, G.J. Mapping Smallholder Maize Farm Distribution Using Multi-Temporal Sentinel-1 Data Integrated with Sentinel-2, DEM and CHIRPS Precipitation Data in Google Earth Engine. *S. Afr. J. Geomat.* **2024**, *13*, 321–351. [CrossRef]
55. Dlamini, L.; Crespo, O.; van Dam, J.; Gaso, D.V.; de Wit, A. Climate Change Impacts on Rainfed Maize Production of Small-Scale Cropping Systems in Eastern Cape, South Africa. *Agric. Syst.* **2026**, *233*, 104627. [CrossRef]
56. Masupha, T.E.; Moeletsi, M.E. Use of Standardized Precipitation Evapotranspiration Index to Investigate Drought Relative to Maize, in the Luvuvhu River Catchment Area, South Africa. *Phys. Chem. Earth* **2017**, *102*, 1–9. [CrossRef]
57. Masupha, T.E.; Moeletsi, M.E. The Use of Water Requirement Satisfaction Index for Assessing Agricultural Drought on Rain-Fed Maize, in the Luvuvhu River Catchment, South Africa. *Agric. Water Manag.* **2020**, *237*, 106142. [CrossRef]
58. Gorelick, N.; Hancher, M.; Dixon, M.; Ilyushchenko, S.; Thau, D.; Moore, R. Google Earth Engine: Planetary-Scale Geospatial Analysis for Everyone. *Remote Sens. Environ.* **2017**, *202*, 18–27. [CrossRef]
59. Drusch, M.; Del Bello, U.; Carlier, S.; Colin, O.; Fernandez, V.; Gascon, F.; Hoersch, B.; Isola, C.; Laberinti, P.; Martimort, P.; et al. Sentinel-2: ESA's Optical High-Resolution Mission for GMES Operational Services. *Remote Sens. Environ.* **2012**, *120*, 25–36. [CrossRef]
60. Segarra, J.; Buchaillot, M.L.; Araus, J.L.; Kefauver, S.C. Remote Sensing for Precision Agriculture: Sentinel-2 Improved Features and Applications. *Agronomy* **2020**, *10*, 641. [CrossRef]
61. Lepot, M.; Aubin, J.B.; Clemens, F.H.L.R. Interpolation in Time Series: An Introductive Overview of Existing Methods, Their Performance Criteria and Uncertainty Assessment. *Water* **2017**, *9*, 796. [CrossRef]

62. Atkinson, P.M.; Jeganathan, C.; Dash, J.; Atzberger, C. Inter-Comparison of Four Models for Smoothing Satellite Sensor Time-Series Data to Estimate Vegetation Phenology. *Remote Sens. Environ.* **2012**, *123*, 400–417. [CrossRef]
63. Chaves, M.E.D.; Alves, M.d.C.; Sáfadi, T.; Oliveira, M.S.d.; Picoli, M.C.A.; Simoes, R.E.O.; Mataveli, G.A.V. Time-Weighted Dynamic Time Warping Analysis for Mapping Interannual Cropping Practices Changes in Large-Scale Agro-Industrial Farms in Brazilian Cerrado. *Sci. Remote Sens.* **2021**, *3*, 100021. [CrossRef]
64. Breiman, L. Random Forests. *Mach. Learn.* **2001**, *45*, 5–32. [CrossRef]
65. Belgiu, M.; Drăgu, L. Random Forest in Remote Sensing: A Review of Applications and Future Directions. *ISPRS J. Photogramm. Remote Sens.* **2016**, *114*, 24–31. [CrossRef]
66. Cortes, C.; Vapnik, V. Support-Vector Networks. *Mach. Learn.* **1995**, *20*, 273–297. [CrossRef]
67. Sheykhmousa, M.; Mahdianpari, M.; Ghanbari, H.; Mohammadimanesh, F.; Ghamisi, P.; Homayouni, S. Support Vector Machine Versus Random Forest for Remote Sensing Image Classification: A Meta-Analysis and Systematic Review. *IEEE J. Sel. Top. Appl. Earth Obs. Remote Sens.* **2020**, *13*, 6308–6325. [CrossRef]
68. Cover, T.M.; Hart, P.E. Nearest Neighbor Pattern Classification. *IEEE Trans. Inf. Theory* **1967**, *13*, 21–27. [CrossRef]
69. Dudani, S.A. The Distance-Weighted k-Nearest-Neighbor Rule. *IEEE Trans. Syst. Man Cybern.* **1976**, *SMC-6*, 325–327. [CrossRef]
70. Chirici, G.; Mura, M.; McInerney, D.; Py, N.; Tomppo, E.O.; Waser, L.T.; Travaglini, D.; McRoberts, R.E. A Meta-Analysis and Review of the Literature on the k-Nearest Neighbors Technique for Forestry Applications That Use Remotely Sensed Data. *Remote Sens. Environ.* **2016**, *176*, 282–294. [CrossRef]
71. Hoerl, A.E.; Kennard, R.W. Ridge Regression: Biased Estimation for Nonorthogonal Problems. *Technometrics* **1970**, *12*, 55–67. [CrossRef]
72. Pedregosa, F.; Varoquaux, G.; Gramfort, A.; Michel, V.; Thirion, B.; Grisel, O.; Blondel, M.; Prettenhofer, P.; Weiss, R.; Dubourg, V.; et al. Scikit-Learn: Machine Learning in Python. *J. Mach. Learn. Res.* **2011**, *12*, 2825–2830. [CrossRef]
73. Naidu, G.; Zuva, T.; Sibanda, E.M. A Review of Evaluation Metrics in Machine Learning Algorithms. In *Artificial Intelligence Application in Networks and Systems*; Lecture Notes in Networks and Systems (LNNS); Springer: Cham, Switzerland, 2023; Volume 724.
74. Kumar, D.A.; Srikanth, P.; Neelima, T.L.; Devi, M.U.; Suresh, K.; Murthy, C.S. Monitoring of Spectral Signatures of Maize Crop Using Temporal SAR and Optical Remote Sensing Data. *Int. J. Bio-Resour. Stress Manag.* **2021**, *12*, 745–750. [CrossRef]
75. Venancio, L.P.; Filgueiras, R.; da Cunha, F.F.; dos Santos Silva, F.C.; dos Santos, R.A.; Mantovani, E.C. Mapping of Corn Phenological Stages Using NDVI from OLI and MODIS Sensors. *Semin. Cienc. Agrar.* **2020**, *41*, 1517–1534. [CrossRef]
76. Tamás, A.; Kovács, E.; Horváth, É.; Juhász, C.; Radócz, L.; Rátonyi, T.; Ragán, P. Assessment of NDVI Dynamics of Maize (*Zea mays* L.) and Its Relation to Grain Yield in a Polyfactorial Experiment Based on Remote Sensing. *Agriculture* **2023**, *13*, 689. [CrossRef]
77. Manimozhian, A.; Chandel, A.K. Phenology-Adaptive Machine Learning for Early Mapping of Field-Scale Corn Crop Yield Using Fusion of Sentinel-2 Satellite Spectral Imagery, and Weather-Based Accumulated Heat Units. *Precis. Agric.* **2026**, *27*, 128. [CrossRef]


**Disclaimer/Publisher's Note:** The statements, opinions and data contained in all publications are solely those of the individual author(s) and contributor(s) and not of MDPI and/or the editor(s). MDPI and/or the editor(s) disclaim responsibility for any injury to people or property resulting from any ideas, methods, instructions or products referred to in the content.